Adhesion Forces between *E. coli* Bacteria and Biomaterial Surfaces

Yea-Ling Ong,[†] Anneta Razatos,[‡] George Georgiou,[‡,§] and Mukul M. Sharma*[,†,‡]

Departments of Petroleum Engineering, Chemical Engineering, and Institute for Molecular & Cell Biology, The University of Texas at Austin, Austin, Texas 78712

Received August 25, 1998. In Final Form: February 4, 1999

Bacterial infection of biomaterial surfaces is an important problem in the biomedical and health industries. The design of materials resistant to infections necessitates an understanding of the forces driving bacterial adhesion. *Escherichia coli* cells were immobilized onto the tip of a standard atomic force microscope (AFM) cantilever, and force measurements were performed by approaching the modified cantilever onto mica, hydrophilic glass, hydrophobic glass, polystyrene, and Teflon. Consistent with prior qualitative observations, we show that bacterial adhesion is indeed enhanced by the surface hydrophobicity of the substrate. The forces of interaction measured with the AFM are compared to those of model predictions based on an extended-DLVO approach. In this model, short-range acid−base and steric interactions are included with the conventional van der Waals attraction and electrostatic components. The theoretical predictions agree well with experimental data for *E. coli* D21f2, a strain whose outer surface consists of lipopolysaccharide molecules with severely truncated carbohydrate chains. However, the adhesive behavior of *E. coli* strains with more complex cell surface structures was found to be more difficult to model because of the possible involvement of steric and bridging effects or specific receptor−ligand interactions that remain to be resolved.

Introduction

Nonbiological materials are commonly employed in medical practice, for example, as joint prostheses, heart valves, vascular catheters, contact lenses, and dentures. Frequently, failure of such devices stems from bacterial biofilm infections, which are extremely resistant to host defense mechanisms and antibiotic treatment. Often, the only solution to an infected implanted device is surgical removal.[1−3] A detailed understanding of the role of the surface properties of both microorganisms and biomaterials in bacterial adhesion is currently lacking. Until recently, bacterial adhesion has been typically evaluated by estimating the number of cells that remain attached to a substrate of interest following a period of incubation and rinsing.[4,5] Results from such experiments are qualitative in nature; therefore, there is an interest in improving techniques studying bacterial adhesion.

Bacterial adhesion to surfaces consists of the initial attraction of the cells to the surface followed by adsorption and attachment. The physiochemical forces that control the initial approach of cells to natural or artificial surfaces are primarily van der Waals, electrostatic, hydration, and hydrophobic interactions. Subsequently, other short-range stereospecific interactions then mediate irreversible adhesion and attachment of the microorganism to a surface.[2,4] Previous bacterial adhesion studies have attempted to correlate adhesion to surface properties of bacterial cells and substrates. In some cases, adhesion was shown to be related to the surface free energy of the bacteria and/or the substratum,[6,7] whereas in other cases, no correlation could be detected.[8,9] Furthermore, DLVO theory, which accounts for long-range van der Waals interactions and electrostatic interactions (attractive or repulsive) resulting from the overlap of electrical double layers, has only been marginally successful in describing interactions of biological systems.[10]

Recently, Razatos et al.[11,12] developed an atomic force microscopy based methodology for directly measuring the forces of interaction between atomic force microscope (AFM) cantilevers with standard silicon nitride (Si_3N_4) tips and bacterial lawns immobilized onto flat glass substrates. When microspheres are glued onto standard Si_3N_4 tips, the probes could be modified to study the interaction of bacteria with various surfaces of interest.[11] However, this technique is limited to the study of materials that can be manufactured into micron-sized beads of low size disparity. Furthermore, the curvature of the beads complicates the quantitative interpretation of the force curves. To address these problems, Razatos et al.[12] developed a procedure for coating the Si_3N_4 AFM cantilever tip with a confluent layer of bacteria. In this configuration, the interaction of the cantilever tip with a substrate is determined solely by the surface features of the attached bacteria. Indeed, it was shown that force curves obtained using bacteria-coated tips and a clean glass surface were experimentally indistinguishable from those obtained by probing a confluent bacterial lawn immobilized on glass with a bare Si_3N_4 tip.[12]

* To whom correspondence should be addressed. E-mail: mukul_sharma@pe.utexas.edu. Tel: (512) 471-3257. Fax: (512) 471-9605.

† Department of Petroleum Engineering.

‡ Department of Chemical Engineering.

§ Institute for Molecular & Cell Biology.

(1) Stickler, D. J.; McLean, R. J. C. *Cells Mater.* **1995**, *5* (2), 167.

(2) Klotz, S. A. In *Microbial Cell Surface Hydrophobicity*; Doyle, R. J., Rosenberg, M., Eds.; American Society for Microbiology: Washington, DC, 1990.

(3) Gristina, A. G. *Science* 1**987**, *237* (4822), 1588.

(4) Ofek, I.; Doyle, R. J. *Bacterial Adhesion to Cells and Tissues*; Chapman Hall Inc.: New York, 1994.

(5) Fletcher, M.; Pringle, J. H. *J. Colloid Interface Sci.* **1985**, *104* (1), 5.

(6) Fletcher, M.; Loeb, G. I. *Appl. Environ. Microbiol.* **1979**, *37*, 67.

(7) Absolom, D. R.; et al. *Appl. Environ. Microbiol.* **1983**, *46* (1), 90.

(8) van Pelt, A. W. J.; Weerkamp, A. H.; Uyen, H. M.; Busscher, H. J.; de Jong, H. P.; Arends, J. *Appl. Environ. Microbiol.* **1985**, *49* (5), 1270.

(9) McEldowney, S.; Fletcher, M. *J. Gen. Microbiol.* **1986**, *132*, 513.

(10) van Oss, C. J. *Colloids Surf. A* **1993**, *78*, 1.

(11) Razatos, A. P.; Ong, Y. L.; Sharma, M. M.; Georgiou, G. *J. Biomater. Sci., Polym. Ed.* in press.

(12) Razatos, A. P.; Ong, Y. L.; Sharma, M. M.; Georgiou, G. Submitted for publication.

10.1021/la981104e CCC: $18.00
Published on Web 03/17/1999

In this paper, we compare the initial force of interaction between bacteria-coated AFM cantilevers and a variety of planar substrates including mica, hydrophilic glass, hydrophobic glass, polystyrene, and Teflon. Our results agree with previous studies[13−15] that bacterial adhesion is indeed strongly influenced by the surface hydrophobicity of the substrate. Experimental results using the AFM to measure the forces of interaction between bacteria and substrates were compared to theoretical predictions based on an extended-DLVO model. In this model, polar (or hydrophobic) and steric interactions were added to the conventional van der Waals attraction and electrostatic components. Theoretical predictions agree well with AFM experimental data for an *Escherichia coli* strain whose surface consists of lipopolysaccharide molecules with short carbohydrate chains. However, the model was not as successful in predicting the adhesive behavior of a genetically related *E. coli* strain whose surface is covered with lipopolysaccharide molecules having longer carbohydrate chains.

Experimental Procedures

Cell Preparation. Isogenic *E. coli* K12 mutant strains differing in the composition of the core carbohydrate moiety of lipopolysaccharide (LPS) coating the cell surface were acquired from the *E. coli* Genetic Stock Center (Department Biology, Yale University, New Haven, CT). Immobilization of bacterial cells onto the microfabricated Si_3N_4 tips requires pretreatment of both the *E. coli* cells and the AFM cantilevers. The wild-type D21 or the mutant D21f2 strains were grown aerobically in Luria Broth at 37 °C. The cells were harvested in exponential phase and washed in phosphate-buffered saline (PBS; 136 mM NaCl, 2.68 mM KCl, 10.1 mM Na_2PO_4, 1.37 mM KH_2PO_4, pH 7.5). The cells were then treated with 2.5 vol % glutaraldehyde (MW = 100.1) for 2.5 h at 4 °C with a final concentration of 0.6−0.8 mg of DCW/mL. After fixation, cells were rinsed copiously, resuspended in 1 mM Tris (tris(hydroxymethyl)aminomethane; Eastman Kodak Co., Rochester, NY), and pelleted by centrifugation at 8000 rpm for 10 min. For cell fixation, a glutaraldehyde solution was prepared by diluting a 25 vol % stock solution (Grade II; Sigma Chemical Co., St. Louis, MO) with PBS and adjusting to pH 7.5. The 2.5 vol % solution was further treated with 50 mg/mL of charcoal at 4 °C for 24 h in order to remove any polymerized glutaraldehyde.[16]

To prepare AFM cantilevers (Nanoprobe−Digital Instruments, Santa Barbara, CA), a drop of poly(ethyleneimmine) (PEI; MW = 1200) solution was allowed to adsorb onto the cantilevers for 2.5 h; the excess liquid was decanted. The cantilevers were subsequently rinsed in distilled, deionized water and stored at 4 °C. The 1% PEI solution was prepared by dilution of a 100% stock solution (Polysciences Inc., Warrington, PA) in distilled, deionized water.[11]

A pellet of cells was manually transferred onto the PEI-coated Si_3N_4 tip, which is the probing side of the cantilever, taking care not to contaminate the side of the cantilever upon which the laser is focused. This was achieved most effectively by using a micromanipulator while viewing the procedure under a microscope. The cell-covered tip was further treated with a drop of glutaraldehyde (2.5 vol %) at 4 °C to strengthen and anchor the pellet onto the tip. After incubation for 1−2 h, the cantilevers were rinsed in distilled, deionized water.

Substrate Preparation. Mica was freshly cleaved prior to use in force measurements. Glass slides were cleaned in H_2O/CrO_3/H_2SO_4 (42:29:29 wt %) for 24 h at room temperature and then rinsed with deionized water. Clean glass slides were made hydrophobic through immersion in 1% octadecyltrichlorosilane (OTS; United Chemical Technologies Inc., Bristol, PA) dissolved in chloroform for 3 h followed by extensive rinsing with water. Polystyrene thin films were prepared by spin-coating 2% polystyrene (MW = 200 000) in a toluene solution onto silicone disks at 2000 rpm. Teflon (Laired Plastics Co., Austin, TX) slabs were cleaned with ethanol followed by deionized water. Using an epoxy glue-hardener mix, the samples were glued onto circular stainless steel magnetic disks which were then mounted on the piezoelectric scanner.

Surface Force Measurements. A Nanoscope III contact mode atomic force microscope (Digital Instruments, Santa Barbara, CA) was used to measure the interactions of isogenic *E. coli* strains with various substrates. Nanoprobe cantilevers with silicon nitride tips were obtained from Digital Instruments (Santa Barbara, CA). Long, thin cantilevers were modified by coating the tips with bacteria as described above. Fresh, new cantilevers were employed for each experiment. All measurements were performed in Tris buffer using an AFM fluid cell (Digital Instruments, Santa Barbara, CA) unless otherwise stated. To prevent contamination, all of the experiments were conducted by engaging the AFM without touching the substrate. The tip was approached to the substrate in 100 nm increments with a scan size of 300 nm. At the end of each measurement, the cantilever was imaged with a scanning electron microscope (SEM) to confirm the presence of a confluent bacterial lawn on the tip.

Data Analysis. Data were acquired in terms of tip deflection (nm) versus piezo position (nm). Multiple curves were plotted together as tip deflection versus relative distance of separation (nm) by aligning their zero deflection regions (flat portion of the curves) and their constant compliance regions (portion of curves where the cantilever moves with the surface).

Tip deflection data were converted to force by first setting the force of interaction to zero where there was no tip deflection and then multiplying by the spring constant of the cantilevers.[17] The spring constant (k) for the long, thin cantilever was $k = 0.06$ nN/nm. Short, thin cantilevers with $k = 0.6$ nN/nm were used to measure the forces of interaction between D21 or D21f2 and OTS-treated glass. Contact between the surface and the tip (zero distance of separation) was defined by the start of the constant compliance region. The distance of separation (nm) was calculated as the sum of the tip deflection and the piezo position relative to zero distance of separation.[17] Plots of force (nN) versus distance of separation (nm) are presented as insets to plots of tip deflection versus relative distance of separation.

Contact Angle Measurements. Contact angles (θ) were measured by the sessile drop technique using a Rame-Hart goniometer. The polar liquids used were water ($\gamma^{LW} = 21.8$ and $\gamma^+ = \gamma^- = 25.5$ mJ m^{-2}) and glycerol ($\gamma^{LW} = 34.0$, $\gamma^+ = 3.92$ mJ m^{-2}, and $\gamma^- = 57.4$ mJ m^{-2}), while the apolar liquid used was diiodomethane ($\gamma^{LW} = 50.8$ and $\gamma^+ = \gamma^- = 0$ mJ m^{-2}).[10,18] For each probe liquid, θ was measured at two locations on three different samples. The standard deviations for contact angles were less than ± 5° for both *E. coli* strains investigated.

Contact angles for bacteria were determined on bacterial lawns created by filtering cells onto porous membranes.[18] Exponential-phase *E. coli* resuspended in 1 mM Tris was vacuum-suctioned onto 0.45 μm cellulose acetate membranes (type HV, Millipore Corp., Bedford, MA) for 10−30 min. When a vacuum is applied, the bacterial cells were compacted into a homogeneous lawn, reducing variation in θ caused by the roughness of the sample, thus preventing permeation of the samples by the sessile drops of liquid. The samples were further exposed to air at room temperature for 5−10 min to evaporate excess residual fluid adhering onto the bacterial lawn. To prevent desiccation of the cells, the membranes were stored in a constant-humidity chamber.

ζ Potential Measurements. ζ potentials were measured for *E. coli* strains resuspended in 1 mM Tris with and without glutaraldehyde treatment using a ζ Reader (model Zr12s;

(13) Zita, A.; Hermansson, M. *FEMS Microbiol. Lett.* **1997**, *152* (2), 299.
(14) van Loosdrecht, M. C. M.; Lyklema, J.; Norde, W.; Schraa, G.; Zehnder, A. J. B. *Appl. Environ. Microbiol.* **1987**, *53* (8), 1893.
(15) Busscher, H. J.; Weerkamp, A. H.; van der Mei, H. C.; van Pelt, A. W. J.; de Jong, H. P.; Arends, J. *Appl. Environ. Microbiol.* **1984**, *48*, 980.
(16) Freeman, A.; Abramov, S.; Georgiou, G. *Biotechnol. Bioeng.* **1996**, *52*, 625.
(17) Ducker, W. A.; Senden, T. J.; Pashley, R. M. *Langmuir* **1992**, *8*, 1831.
(18) van Oss, C. J.; Good, R. J.; Chaudhury, M. K. *J. Colloid Interface Sci.* **1986**, *111*, 378.

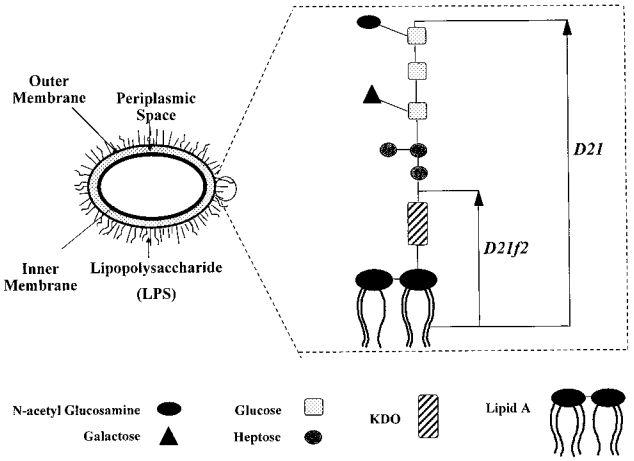

Figure 1. Core lipopolysaccharide (LPS) structure of *E. coli* K12 mutant strain D21f2 and its parental strain D21 which synthesizes the complete carbohydrate chain.

Komline Sanderson, Peapack, NJ). ζ potential values for planar substrates (i.e., polystyrene, glass, etc.) were taken from the literature.[19,20]

Experimental Results

The model organism used in this study is *E. coli*. The outermost surface of *E. coli* and other Gram-negative bacteria is defined by the outer membrane, an asymmetric lipid bilayer whose external lipid component consists exclusively of LPS. For K12 strains of *E. coli*, the LPS molecule consists of a lipid moiety (lipid A) linked to a carbohydrate chain of variable length (Figure 1). In this work, *E. coli* D21 synthesizes LPS, expressing the entire core carbohydrate chain that extends 20 Å from the lipid bilayer.[21] D21f2 is an isogenic mutant strain that is genetically identical to the parent D21 strain except for a genetic mutation in the biosynthesis of LPS, resulting in a severely truncated core carbohydrate chain (Figure 1).[22]

To perform AFM measurements, it was necessary to establish a reliable and mild procedure for the formation of a confluent cell layer on the cantilever tip. *E. coli* cells were treated with glutaraldehyde and subsequently immobilized onto PEI-coated Si_3N_4 tips. Scanning electron micrographs taken at the end of force measurements revealed that the Si_3N_4 tip remained covered with a confluent layer of bacteria. In Figure 2, an AFM cantilever with a microfabricated Si_3N_4 tip is shown next to a tip coated with *E. coli* cells.

We have conducted a number of control experiments to verify that the protocol for cell immobilization did not introduce experimental artifacts. First, Razatos et al.[11] demonstrated that the force curves obtained for molecularly smooth mica using a fresh, clean cantilever versus a cantilever that had been incubated over glass precoated with PEI were identical, indicating that PEI does not desorb off of the support surface to contaminate the tip. Second, Razatos et al.[12] showed that contact angle and ζ potential measurements of bacterial cells were identical

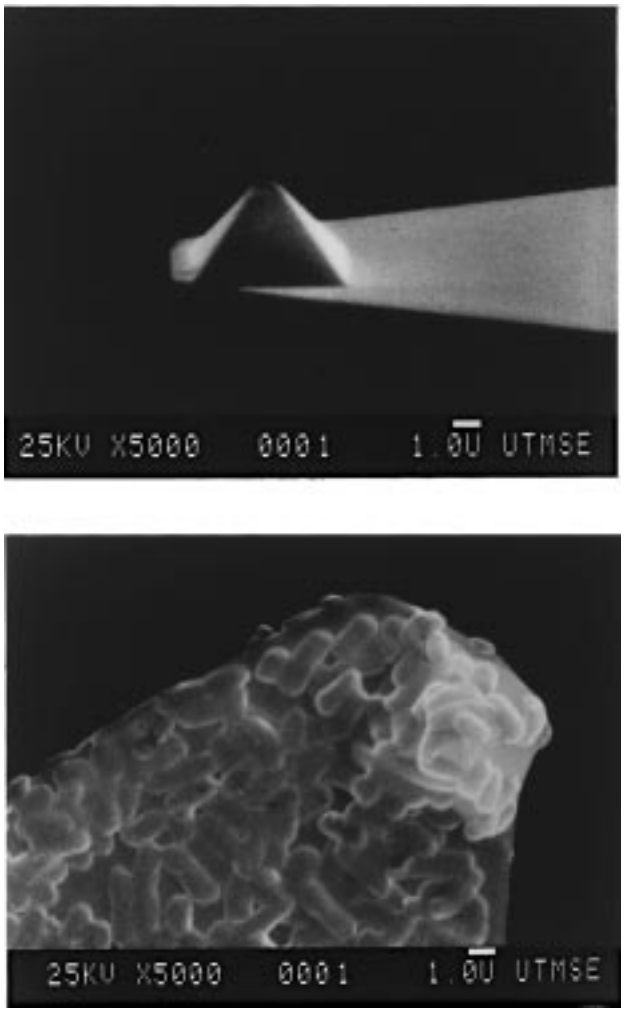

Figure 2. SEM micrographs of a standard AFM cantilever with a microfabricated Si_3N_4 tip and a cantilever tip coated with *E. coli* D21 cells.

before and after glutaraldehyde fixation. Moreover, force curves measured for both D21f2 and D21 treated with different concentrations of glutaraldehyde (1.5−5 vol %) over different periods of time (2.5−3.5 h) were identical (data not shown). Glutaraldehyde fixation with 2.5 vol % for 2.5 h was most efficient in producing stable bacterial coatings on Si_3N_4 tips. For biological specimens, glutaraldehyde is frequently used as a fixative. Glutaraldehyde cross-links the amines in cellular proteins, thus enhancing the structural integrity and rigidity of biological samples.[23,24] LPS molecules which coat *E. coli* cells lack free amines and, therefore, are not chemically modified by the glutaraldehyde treatment. These results indicate that the use of glutaraldehyde does not affect the physiochemical properties of the bacterial cell surface involved in interactions with surfaces.

AFM Results. AFM cantilevers coated with bacteria were used to measure the force of interaction between cells and various materials. On the basis of contact angle measurements (Table 1), the surfaces investigated were mica, glass, polystyrene spun films, and Teflon listed in order of increasing hydrophobicity. Force measurements obtained with the AFM are readily reproducible.[11,12] All force curves represent averages of at least three independent experiments using new cantilevers for every force measurement.

(19) Uyen, H. M.; van der Mei, H. C.; Weerkamp, A. H.; Busscher, H. J. *Appl. Environ. Microbiol.* **1988**, *54* (3), 837.
(20) van Loosdrecht, M. C. M.; Lyklema, J.; Norde, W.; Schraa, G.; Zehnder, A. J. B. *Appl. Environ. Microbiol.* **1987**, *53* (8), 1898.
(21) *Escherichia coli and Salmonella typherium: Cellular and Molecular Biology*; Neidhardt, F. C., Curtis, R., III, Ingraham, J. L., Lin, E. C., Low, K. B., Magasanik, B., Reznikoff, W. S., Riley, M., Schaechter, M., Umbarger, H. E., Eds.; ASM Press: Washington, DC, 1990.
(22) Boman, H. G.; Moner, D. A. *J. Bacteriol.* **1975**, *121* (2), 455.
(23) Hoh, J. H.; Schoenenberger, C. A. *J. Cell Sci.* **1994**, *107*, 1105.
(24) Schoenenberger, C. A.; Hoh, J. H. *Biophys. J.* **1994**, *67*, 929.

Table 1. Characterization of Interacting Surfaces via Contact Angle Measurements

	θ_{Water}	$\theta_{Glycerol}$	θ_{DI}
substrate			
mica	0	11.1 ± 0.9	31.8 ± 0.7
glass	14.2 ± 0.8	8.5 ± 0.8	34.5 ± 1.1
OTS−glass	94.9 ± 1.6	92.5 ± 0.6	60.6 ± 1.6
polystyrene	74.3 ± 1.8	73.7 ± 0.8	29.8 ± 0.7
Teflon	110.6 ± 0.7	100.8 ± 0.8	77.4 ± 0.7
E. coli D21f2	31.4 ± 4.0	43.2 ± 2.5	67.0 ± 2.6
E. coli D21	19.3 ± 3.0	36.0 ± 2.6	61.1 ± 2.4

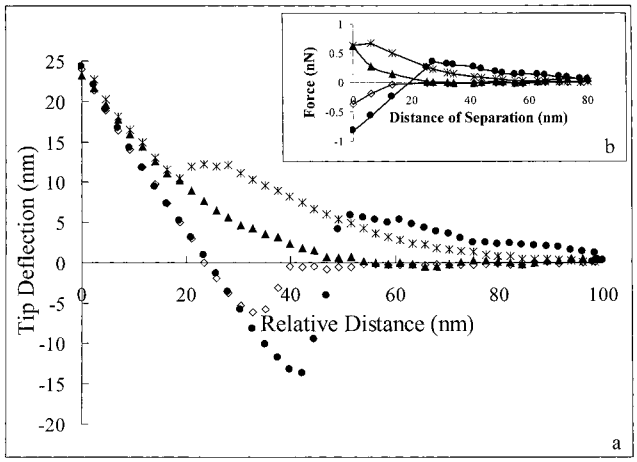

Figure 3. Interaction of AFM tips coated with *E. coli* D21f2 and various substrates presented as (a) tip deflection vs relative distance of separation and (b) force vs distance of separation. Measurements were performed in 1 mM Tris (pH 7.5). Legend: *, mica; ▲, glass; ◇, polystyrene; ●, teflon.

The tip deflection and force curves for the mutant D21f2 interacting with various substrates are presented in parts a and b of Figure 3, respectively. Upon approaching mica, D21f2 cells experienced a strong repulsive force. On glass, the same trend is observed although the magnitude of the repulsive interaction is weaker. In its interaction with mica, D21f2 has to overcome a greater energy barrier, as shown by the jump in the curve. The repulsion of D21f2 on both substrates appears to be dictated by electrostatic interactions (see below). In contrast, D21f2 was attracted to both polystyrene and Teflon, with the attraction for the latter surface being significantly stronger. Because the Teflon is more hydrophobic, it appears that increasing substrate hydrophobicity results in stronger cell adhesion. A similar increase in bacterial adhesion with surface hydrophobicity has been observed previously for a number of different strains.[13,14]

Tip deflection and force curves demonstrating the behavior of the parental *E. coli* strain D21 are illustrated in parts a and b of Figure 4, respectively. When Figures 3 and 4 are compared, it is interesting to note that D21 and D21f2 displayed quite the opposite behavior in their interaction with each substrate. These differences are statistically significant, and the discrepancy is reproducible in all instances. For example, while D21f2 was repelled by both mica and glass, D21 was attracted to both substrates. Conversely, D21 displayed a net repulsion for polystyrene and Teflon, whereas D21f2 experienced an attractive interaction.

Experiments with both *E. coli* strains on mica were repeated in a 1 mM Tris plus 100 mM NaCl solution (Figure 5). Upon addition of NaCl to the Tris buffer, the repulsion between D21f2 and mica was reduced. The ions screen the surface charges, lowering the repulsive potential experienced between the two negatively charged

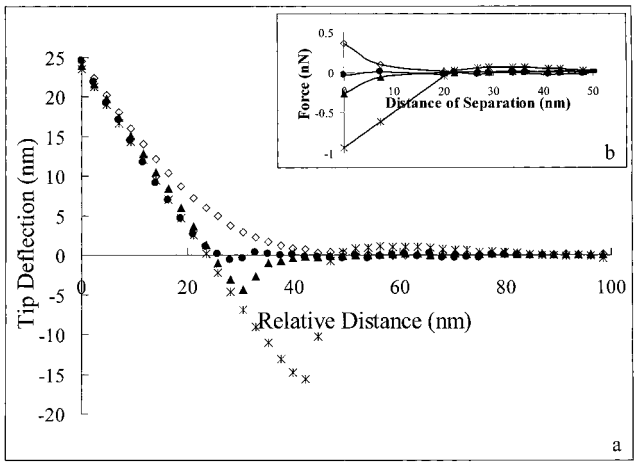

Figure 4. Interaction of AFM tips coated with *E. coli* D21 and various substrates presented as (a) tip deflection vs relative distance of separation and (b) force vs distance of separation. Measurements were performed in 1 mM Tris (pH 7.5). Legend: *, mica; ▲, glass; ◇, polystyrene; ●, teflon.

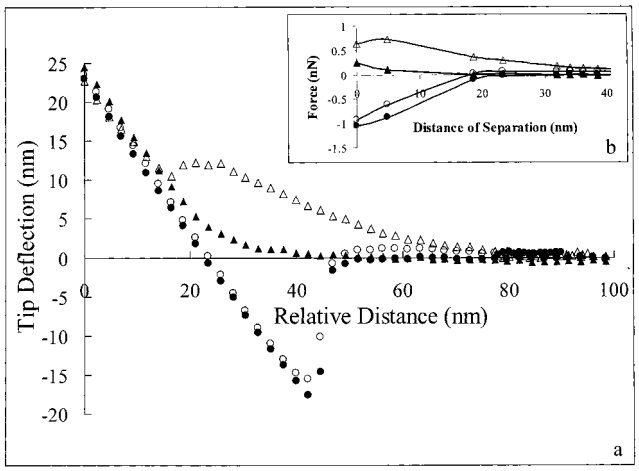

Figure 5. Interaction between AFM tips coated with *E. coli* D21f2 or D21 and mica in 1 mM Tris and 1 mM Tris plus 100 mM NaCl. Curves are presented as (a) tip deflection vs relative distance of separation and (b) force vs distance of separation. Legend: △, D21f2 in 1 mM Tris; ▲, D21f2 in 1 mM Tris + 100 mM NaCl; ○, D21 in 1 mM Tris; ●, D21 in 1 mM Tris + 100 mM NaCl.

surfaces. The attraction between D21 and mica with the addition of 100 mM NaCl, however, remained statistically identical to the attraction observed in Tris buffer alone. Similar trends were observed when bacterial lawns were probed with a standard Si_3N_4 tip in deionized water, Tris, and Tris plus NaCl.[12] Therefore, the repulsive force, which is strongly influenced by the salinity of the liquid medium,[25,26] is electrostatic in nature.

The effect of material surface hydrophobicity on adhesion was further investigated by examining the interaction of *E. coli* cells with clean glass and glass with a hydrophobic coating. Glass surfaces were cleaned with a strong acid and then rendered hydrophobic by coating with OTS. On the clean, hydrophilic glass surface, D21f2 was mildly repelled while D21 showed a weak attraction (Figure 6a). However, on the hydrophobic glass surface, both bacterial strains experienced attractive forces that were so large that the AFM cantilevers used in all previous experiments

(25) Butt, H. J. *Biophys. J.* **1991**, *60* (4), 777 and 1438.
(26) Israelachvili, J. *Intermolecular & Surface Forces,* 2nd ed.; Academic Press: San Diego, 1991.

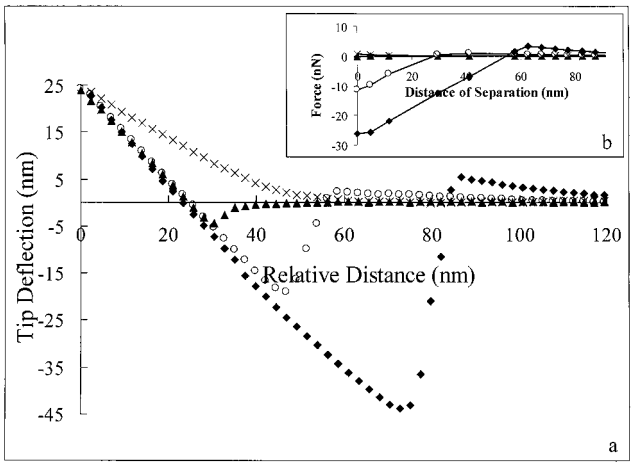

Figure 6. Force measurements obtained for hydrophilic glass substrate using bacteria-coated AFM cantilevers with a spring constant of $k = 0.06$ N/m. For hydrophobic OTS-treated glass, stiffer cantilevers with a spring constant of $k = 0.60$ N/m were used. All measurements were performed in 1 mM Tris (pH 7.5). Curves are presented as (a) tip deflection vs relative distance of separation and (b) force vs distance of separation. Legend: ×, D21f2 on hydrophilic glass; ◆, D21f2 on OTS-treated glass; ▲, D21 on hydrophilic glass; ○, D21 on OTS-treated glass.

were not stiff enough to measure the force of interaction (Figure 6a). For this reason, experiments on OTS-treated glass were performed using cantilevers with larger spring constants in comparison to cantilevers used in previous experiments (0.60 vs 0.06 N/m). The forces of interaction calculated for D21 and D21f2 interacting with clean glass and OTS-treated glass are presented in Figure 6b.

Discussion

The bacterial strains used in this study are genetically identical except for a mutation in the biosynthetic pathway of LPS. As a result the D21 strain expresses the full LPS core carbohydrate chain whereas the mutant strain, D21f2, expresses an LPS molecule having a shorter core carbohydrate chain (Figure 1). Force measurements on a variety of substrates show that the LPS molecules coating the cell surface greatly influence bacterial adhesion. According to contact angle and ζ potential measurements (Tables 1 and 2), cells with truncated LPS molecules (D21f2) express a stronger net negative surface charge to their environment and are considered to be relatively more hydrophobic. D21f2 is strongly repelled by the hydrophilic, negatively charged surfaces of glass and mica (Figure 3). AFM experiments performed in higher electrolyte concentrations (Figure 5) reveal that this repulsive behavior is, in fact, electrostatic in nature. However, in addition to electrostatic interactions, the hydrophobic effect also plays a significant role in bacterial adhesion. The attractive force for the more hydrophobic D21f2 strain increases with respect to hydrophobicity of the substrate (mica < glass < polystyrene < Teflon), as seen in Figure 3. The importance of hydrophobic interactions in bacterial adhesion is clearly illustrated in Figure 6, where D21f2 was strongly attracted to hydrophobic OTS-treated glass but was repelled by hydrophilic glass. In agreement with these results, strong attractive forces have been reported for the interaction between clean glass spheres and OTS-treated glass substrates.[27]

In summary, we observe that the adhesion of relatively hydrophobic cells (D21f2) is favored on low-energy substrates (Figure 3). Conversely, the adhesion of the more hydrophilic or high surface energy cells (D21) is favored on high-energy substrates such as glass and mica (Figure 4). Here, the attractive behavior observed between D21 is not affected by the addition of salt and, therefore, is not electrostatic in origin (Figure 5). This attraction could be due to van der Waals interactions or bridging effects,[19] mediated by the long LPS tails. Further, it should be recognized that hydrophobic interactions do play a role in adhesion of hydrophilic particles to hydrophobic surfaces.[28] A stronger attraction was observed between D21 and hydrophobic OTS-treated glass in comparison to hydrophilic glass (Figure 6).

Table 2. Surface Tension Components and Hydrophilicity of Various Substrates Expressed as ΔG_{iwi} (mJ m^{-2})

	γ^{LW}	γ^+	γ^-	ΔG_{iwi}
mica	43.45	2.30	46.31	17.41
glass	42.25	2.90	42.00	12.44
OTS−glass	28.24	0.43	7.32	−42.00
polystyrene	44.31	0.46	2.22	−70.18
Teflon	18.86	0.01	0.01	−98.39

For hydrophilic surfaces at large distances of separation, the DLVO model which incorporates van der Waals and electrostatic forces agrees with experimental data.[29] However, at small separation distances, steric, solvation, or other specific short-range interactions become important. It is well-documented[10,26] that, in biological systems, DLVO interactions provide poor agreement with experimental observations. McEldowney and Fletcher[30] and others[10,19,20,31] have noted that this approach must be augmented with short-range surface forces to adequately predict cell adhesion.

To understand the contribution of short-range hydration, acid−base, and steric interactions, it is instructive to quantify the surface forces acting between the cells and the substrate. Inclusion of these short-range interactions can be empirically achieved by measuring the change in surface energies at contact. The surface free energies can be derived from contact angle (θ) measurements. According to van Oss et al.,[10,18] the surface free energies can be separated into an apolar or dispersion component (due to Lifshitz−van der Waals forces) and a polar or Lewis acid−base component comprising an electron-donor and electron-acceptor parameter.

$$(1 + \cos\theta)\gamma_i = 2\sqrt{\gamma_i^{LW}\gamma_j^{LW}} + 2\sqrt{\gamma_i^+\gamma_j^-} + 2\sqrt{\gamma_i^-\gamma_j^+} \quad (1)$$

Contact angle (θ) measurements for the different substrates and bacterial lawns using three probe liquids (water, glycerol, and diiodomethane) are shown in Table 1. γ^{LW}, γ^+, and γ^- parameters calculated for the various substrates and *E. coli* cells are shown in Tables 2 and 3, respectively. ΔG_{iwi} values were computed for each surface (i) as a measure of its hydrophilicity. The substrates show a range of hydrophobicities, with Teflon being the most hydrophobic. Further, D21f2 is seen to be slightly more hydrophobic than D21 because of its truncated LPS molecules.

(27) Yoon, R. H.; Flinn, D. H.; Rabinovich, Y. I. *J. Colloid Interface Sci.* **1997**, *185*, 363.

(28) Ducker, W. A.; Zhenghe, X.; Israelachvili, J. N. *Langmuir* **1994**, *10*, 3279.

(29) Pashley, R. M.; Israelachvili, J. *J. Colloid Interface Sci.* **1984**, *97*, 446.

(30) McEldowney, S.; Fletcher, M. *Appld. Environ. Microbiol.* **1986**, *52* (3), 460.

(31) Mozes, N.; Marchal, F.; Hermesse, M. P.; van Haecht, J. L.; Reuliaux, L.; Leonard, A. J.; Rouxhet, P. G. *Biotechnol. Bioeng.* **1987**, Vol. XXX, 439.

Table 3. Surface Tension Components and Hydrophilicity of *E. coli* Strains Expressed as ΔG_{iwi} (mJ m^{-2})

	γ^{LW}	γ^+	γ^-	ΔG_{iwi}
D21f2	24.56	2.62	51.31	28.85
D21	27.92	2.59	56.50	33.19

Table 4. Nonretarded Hamaker Constants A_{132} (10^{-21} J) for the Interaction of *E. coli* in Water

	D21f2	D21
mica	1.04	2.23
glass	0.98	2.12
polystyrene	1.07	2.30
Teflon	−0.18	−0.38

For a bacterium interacting with a substrate, the disjoining pressure (Π_{Total}) for the extended-DLVO model is

$$\Pi_{Total} = \Pi_{Born} + \Pi_{VDW} + \Pi_{EL} + \Pi_{AB} \quad (2)$$

Here, the expression for Born repulsion is obtained by integrating the repulsive part of the Lennard-Jones potential[26,32]

$$\Pi_{Born} \approx \frac{A_{132}\sigma^6}{7560}\left(\frac{168}{\pi h^9}\right) \quad (3)$$

where $A_{132} = -12\pi h_0^2 \Delta G_{132}^{LW}(h_0)$.

The retarded van der Waals expression proposed by Gregory[33] and the electrostatic component computed from the weak overlap approximation[26] have been used. The polar or Lewis acid−base (AB) forces due to electron donor−acceptor interactions are computed from expressions proposed by van Oss et al.[18] and Good et al.[34] The decay with distance (h) for each component is

$$\Pi_{VDW} = \frac{-A_{132}(15.96h/\gamma + 2)}{12\pi h^3(1 + 5.32h/\gamma)^2} \quad (4)$$

$$\Pi_{EL} = 64kT\rho_\infty \tanh\left(\frac{ze\zeta_1}{4kT}\right)\tanh\left(\frac{ze\zeta_2}{4kT}\right)\exp(-\kappa h) \quad (5)$$

$$\Pi_{AB} = \Delta G^{AB}(h_0)\exp\left(\frac{-h}{\lambda}\right) \quad (6)$$

Values for A_{132}, the Hamaker constant for the various bacterium−water−substrate systems, were calculated from experimental values of the apolar surface tension components (γ_i^{LW})[35,36] and are presented in Table 4. The polar free energy $\Delta G_{132}^{AB}(h_0)$ contributions were calculated from experimental values of the polar surface tension components (γ_i^+ and γ_i^-) according to van Oss.[35] The minimum equilibrium distance between the surfaces is set at $h_0 = 0.157 \pm 0.009$ nm, and the decay length $\lambda \approx 0.6-1.0$ nm.[35] σ is the collision diameter, γ is the London wavelength (~1000 Å), ζ_i refers to the ζ potential for the two interacting surfaces (Table 5), and $1/\kappa$ is the Debye length.

The disjoining pressure between two planar surfaces is transformed to accommodate interactions between a sphere and a planar surface using the Derjaguin[37] approximation

$$F/R = 2\pi W_{Total} = 2\pi\int_h^\infty -\Pi\, dh \quad (7)$$

where F refers to the force between a spherical particle of radius R and a planar surface and W is the potential energy of interaction per unit area. This disjoining pressure term, F/R is plotted against the distance of separation in order to predict the adhesive or repulsive behavior of bacteria and surfaces.

Table 5. ζ Potential (mV) of the Interacting Surfaces in 1 MM PBS

	ζ
substrate	−120
mica	
glass	−85
polystyrene	−47.5
Teflon	−43.6
E. coli D21f2	−36.4 ± 4.0
E. coli D21	−28.8 ± 1.7

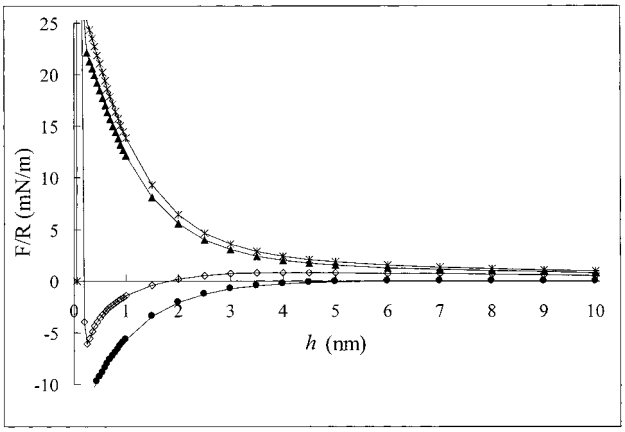

Figure 7. Theoretical force (F/R) versus distance (h) curves for D21f2 based on the augmented DLVO model (eq 2). Legend: *, mica; ▲, glass; ◇, polystyrene; ●, teflon.

Figure 7 presents the forces of interaction (F/R) computed from the augmented DLVO model between *E. coli* D21f2 and the various substrates under investigation. These theoretical force curves in terms of F/R can be compared only qualitatively to experimental force curves in terms of F. For nonspherical, nonrigid particles, R represents the radius of curvature of the contact area. At the present time, for the bacterial lawns investigated in this study, the radius of curvature of the contact area is unkown. During force measurements with the AFM, the substrate is interacting with asparities on the bacterial cell surface and not the bacterial cell surface itself. Therefore, the effective radius of curvature of the contact region is smaller than the radius of curvature of the bacterium and cannot be accurately estimated.

According to the augmented DLVO model (Figure 7), the interaction of D21f2 with synthetic polymers favors adhesion, whereas repulsive behavior is predicted for the interaction of D21f2 with both mica and glass. The free energy of adhesion increases in direct correlation with increasing substrate hydrophobicity. We observed experimentally (Figure 3) that D21f2 was strongly repelled by mica, the most hydrophilic substrate; the repulsion was weaker with glass; an attractive force was observed upon approaching both polystyrene and Teflon, with the strongest adhesion detected for the most hydrophobic substrate. Therefore, both modeling and experimental

(32) Ruckenstein, E.; Prieve, D. C. *AIChE J.* **1976**, *22*, 276.
(33) Gregory, J. *J. Colloid Interface Sci.* **1981**, *83* (1), 138.
(34) Good, R. J.; Chaudhury, M. K.; van Oss, C. J. In *Fundamentals of Adhesion*; Lee, L. H., Ed.; Plenum Press: New York, 1991.
(35) van Oss, C. J. *Colloids Surf. B* **1995**, *5*, 91.
(36) Israelachvili, J. *Quart. Rev. Biophys.* **1974**, *6*, 341.
(37) Derjaguin, B. *Kolloid Z.* **1934**, *69*, 155.

results agree that higher energy hydrophilic surfaces (mica and glass) show a strong monotonic repulsion, whereas hydrophobic substrates with lower surface energies show an attractive minimum for D21f2.

Qualitatively, the modeling results for D21 are similar to those portrayed in Figure 7 for D21f2. However, where the model implies adhesion for D21 to the synthetic hydrophobic polymers, repulsive forces were detected with the AFM. Likewise, when the model predicted repulsion to hydrophilic surfaces, D21 was seen to adhere to both glass and mica. As a result, the model cannot be used to simulate the adhesive behavior as determined experimentally by the AFM for the D21 strain. One reason for the discrepancy between theory and experimental data may be due to steric interactions. If electrostatic or steric effects present a sufficiently large energy barrier, contact between the interacting surfaces is prevented, and as a result the measured adhesion energy will not agree with calculations based on changes in surface free energies measured at contact.[38] The surface of *E. coli* D21 consists of LPS molecules with long carbohydrate chains that would introduce a steric component. Steric effects could result from LPS chains on the bacterial cell surfaces interacting with polymer chains that are reported to radiate from polystyrene surfaces.[39] In an effort to more accurately predict interactions between biological particles and planar surfaces, an expression developed by de Gennes[40] that includes steric interactions between surfaces containing a high density of grafted polymer chains was added to eq 2

$$\Pi_{\text{Steric}} = \frac{kT}{S^3}\left[\left(\frac{2L}{h}\right)^{9/4} + \left(\frac{h}{2L}\right)^{3/4}\right] \qquad (8)$$

where L is the thickness of the brush layer and s, the average distance between anchoring sites, is 0.8 nm. This equation gives the interaction force for separation distances h smaller than twice the thickness of the polymer layer ($2L$).

Figure 8 shows the computed force versus distance curves on polystyrene, with and without accounting for steric effects (Π_{Steric}). The inclusion of steric interactions leads to an additional repulsive component for D21, the wild-type *E. coli* strain expressing long LPS molecules on its cell surface. The interaction curve is modulated, resulting in a net repulsion which is consistent with experimental observations for D21 (Figure 4). For D21f2, however, it is seen that the addition of steric interactions still gives rise to a net attraction to the polymers. D21f2 has been shown to be more hydrophobic than its D21 counterpart. Because attractive hydrophobic (or Lewis acid−base) interactions are known to dominate biological interactions,[35] presumably the total attractive force is sufficient to overcome the steric repulsive component for D21f2.

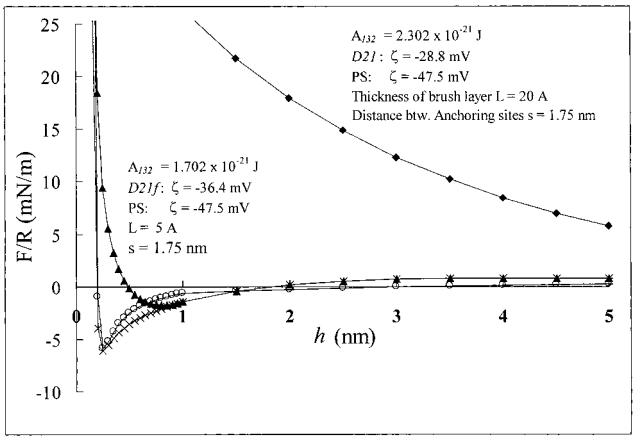

Figure 8. Theoretical force−distance curves incorporating steric effects into an augmented DLVO model for *E. coli* D21f2 and D21 interacting with polystyrene. Legend: ×, D21f2, extended-DLVO model; ▲, D21f2, extended-DLVO model + steric effects; ○, D21, extended-DLVO model; ◆, D21, extended-DLVO model + steric effects.

Conclusions

Atomic force microscopy can be employed to measure the force of interaction between bacteria and any planar surface of interest. This method was successful in elucidating the contribution of LPS molecules to bacterial adhesion. Hydrophobic interactions were found to play a dominant role in the adhesion of two genetically similar *E. coli* strains differing only in LPS composition and thus in overall cell surface charge and hydrophobicity. Moreover, the adhesion process is very sensitive to the physiological properties of the bacterium and the substrate, as well as environmental factors such as electrolyte concentration. An augmented DLVO model incorporating both hydrophobic and steric interactions was developed to model bacterial adhesion as monitored by atomic force microscopy. This model was found to qualitatively agree with experimental data for adhesion of the *E. coli* strain synthesizing truncated LPS molecules. Agreement of the theoretical model with experimental observation suggests that cell adhesion results from an interplay of van der Waals, electrostatic, and hydrophobic interactions. Steric interactions at least partially account for the discrepancies between the model and experimental results observed for *E. coli* D21 expressing long LPS molecules. Other factors such as bridging effects or specific receptor−ligand interactions may also be involved and will need to be accounted for in detail.

Acknowledgment. This work was supported by a grant from the EPA (Grant No. R821 268-01-0) to G.G. and M.M.S. A.R. is a Whitaker Foundation graduate fellow. We are also grateful to Dr. A. Freeman (Tel Aviv University) for his advice on bacterial immobilization and to Dr. P. Green (The University of Texas) for his help with spin-coating thin polymer films.

LA981104E

(38) Frietas, A. M.; Sharma, M. M. Submitted for publication.
(39) Seebergh, J. E.; Berg, J. C. *Colloids Surf. A* **1995**, *100*, 139.
(40) de Gennes, P. G. *Adv. Colloid Interface Sci.* **1987**, *27*, 189.